Basic Dykes Crosscutting the Crystalline Basement of Valsugana (Italy): New Evidence of Early Triassic Volcanism in the Southern Alps

G. Bianchini[1], C. Natali[1], T. Shibata[2,3] and M. Yoshikawa[2]

[1] Department of Physics and Earth Sciences, University of Ferrara, Italy.

[2] Institute for Geothermal Sciences, Kyoto University, Beppu, Japan.

[3] Department of Earth and Planetary Systems Science, Hiroshima University, Higashi-Hiroshima, Japan.

Corresponding author: Claudio Natali (ntlcld@unife.it)

Key Points:

- The studied basic dykes in the south-Alpine reveal Early Triassic age and subduction-related affinity.
- Prevalent shoshonitic affinity suggests significant recycling of crustal components in their mantle sources.
- Magma genesis plausibly occurred in post-collisional setting, following Variscan subduction(s) and continental collision(s)

Abstract

Basic dykes crosscutting the crystalline basement in Valsugana (Southern Alps, Italy) have been investigated for the first time in the framework of the known tectonomagmatic cycles. Petrographic observations and bulk rock analyses suggest a serial affinity variable between calcalkaline (subordinate) to shoshonitic (prevalent), which are generally ascribed to a convergent plate setting. This is confirmed by Sr-Nd-Pb isotopic analyses that display extreme values that are often observed in post-collisional settings. K-Ar dating, available for two samples, yield ages of 236±6 and 251±7 Ma, suggesting that these dykes represent a transition between the Permian and the Triassic volcanic episodes that are known in neighbouring sectors of the Southern Alps. Considering that Permo-Triassic active subduction beneath the South Alpine is scarcely constrained, we ascribe the metasomatism of the related mantle sources to the Variscan cycle, proposing that magma genesis was delayed respect to time of the active subduction(s). According to recent reconstructions, parts of south-eastern Europe, including the South-Alpine domain, were formed by the break-up of the northern Gondwana margin from the Late Cambrian, in connection with important transtensional movements, leaving rifted continental basins or narrow oceanic seaways. In our view, the subduction processes that induced metasomatism in mantle sources of the South-Alpine region occurred in the connection with the subsequent (Carboniferous?) consumption of lithosphere of these basins, a framework that is compatible with pervasive recycling of continental crust components within the mantle wedge. Then, calcalkaline/shoshonite magmatism was triggered in the Early Triassic by post-collisional extensional tectonics that followed the Variscan orogenic cycle.

1 Introduction

The Southern Alps in the Province of Trento (Italy) are constituted by a Paleozoic crystalline basement covered by Mesozoic sedimentary units. Volcanism is also represented, as testified by Permian (calcalkaline products, mainly rhyolitic in composition), Triassic (basic to intermediate shoshonitic products) and Paleogene (tholeiitic and Na-alkaline basalts) episodes. In this framework, the updated 1:50,000 geological map of Trento (http://www.isprambiente.gov.it/Media/carg/60_TRENTO/Foglio.html) revealed in Valsugana (a lateral valley respect to the main Adige valley) the presence of a series of basic dykes (evidenced by green colour and labelled "fy" in the mentioned map) crosscutting the crystalline basement, that are difficult to be addresses to the above mentioned magmatic cycles. In the legend of the map it is specified that they cut the Permian magmatic rocks and therefore it is inferred that they are younger, and as stated at page 111 of the relative notes (http://www.isprambiente.gov.it/Media/carg/note_illustrative/60_Trento.pdf) the Authors attributed the whole spectrum of these dykes to a hypothetic "alpine magmatism". This interpretation was probably influenced by the study of a single magmatic occurrence known as the lamprophyre of Calceranica, which was dated as Upper Cretaceous (71 ± 2 Ma) by Galassi et al. (1994). To crosscheck this hypothesis we collected new samples from dykes located close to the towns of Pergine and Levico and carried out petrographic investigation and major and trace element bulk rock analyses. Moreover, in order to provide further constraints we carried out carbon (C) and strontium (Sr), neodymium (Nd) and lead (Pb) isotopic analyses, as well as K-Ar datings.

2 Materials and Methods

Dykes were localized using the updated 1:50,000 geological map of Trento and sampling sites are reported in Fig. 1.

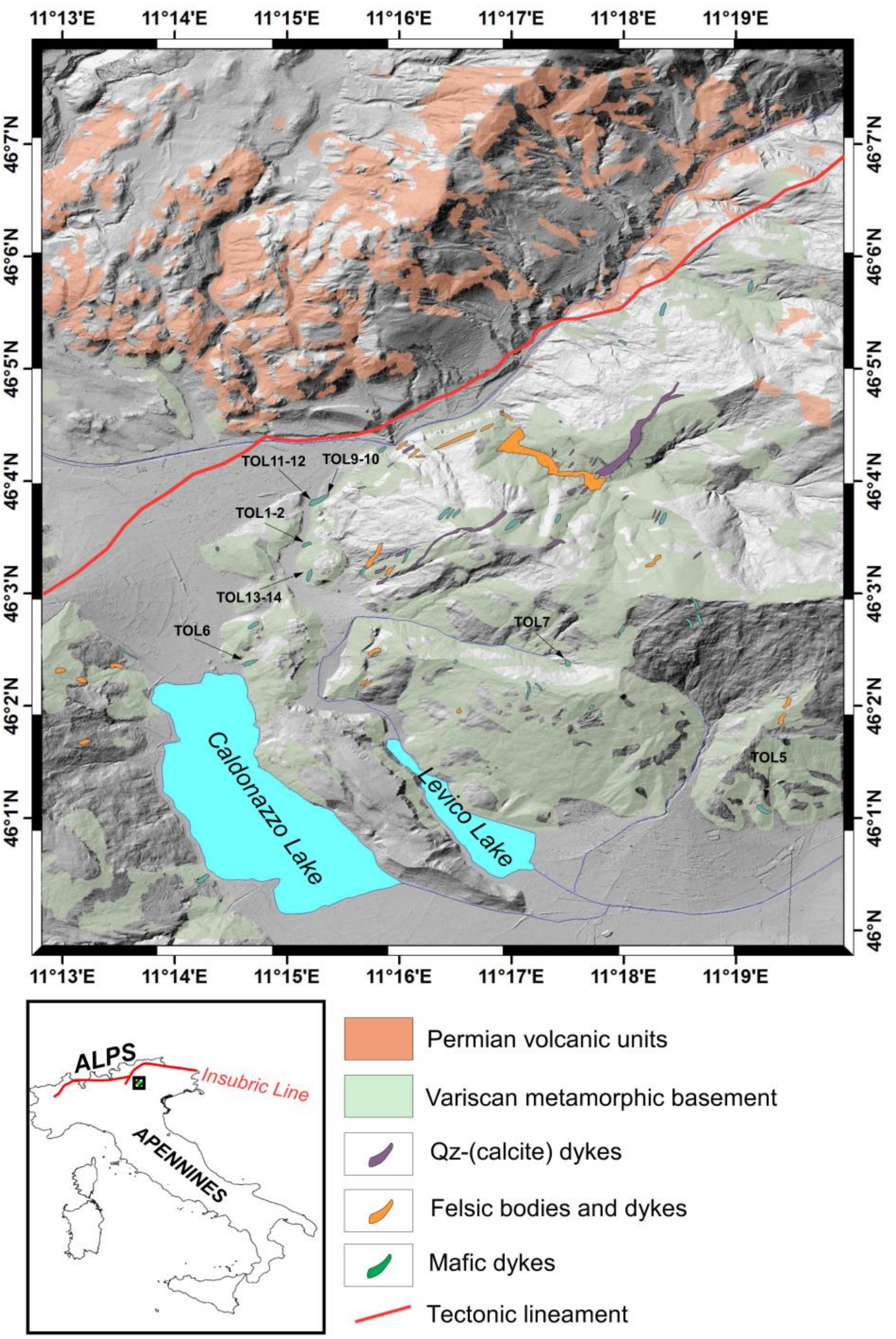

Figure 1. Geological sketch map of the sector of Valsugana where the studied basic dykes outcrop separately.

Specimens were cut in order to remove altered portions and then grinded and powdered in an agate mill. Major and trace elements (Ni, Co, Cr, V, Rb, Sr, and Ba) were analysed by X-ray fluorescence (XRF) on powder pellets, using a wavelength-dispersive automated ARL Advant'X spectrometer at the Department of Physics and Earth Sciences at the University of Ferrara. Accuracy and precision for major elements are estimated as better than 3% for Si, Ti, Fe, Ca, and K, and 7% for Mg, Al, Mn, Na; for trace elements (above 10 ppm) they are better than 10%. REE, Y, Zr, Hf, Nb, Th, and U were analysed, after acid digestion, by inductively coupled mass spectrometry (ICP-MS) at the Department of Physics and Earth Sciences of the University of Ferrara, using a Thermo-Scientific X-Series. Accuracy and precision, based on the replicated analyses of samples and standards, are estimated as better than 10% for all elements, well above the detection limit. Mineral compositions were measured by electron microprobe at the Department of Earth Sciences at the University of Milano with a wavelength dispersive system JEOL 8200 Superprobe (fitted with 5 wavelength dispersive spectrometers) set with an accelerating voltage of 15 kV and specimen current of 20 nA, using natural silicates and oxides as standards. C elemental and isotopic analyses have been carried out on bulk rock powders using a Vario Micro Cube Elemental Analyzer (EA) coupled with an Isoprime 100 Isotope Ratio Mass Spectrometer (IRMS) at the Department of Physics and Earth Science of the University of Ferrara. The elemental precision estimated by repeated standard analyses and accuracy estimated by the comparison between reference and measured values were in the order of 5% of the absolute measured value. Uncertainties increase for contents approaching the detection limit (0.001 wt.%). Carbon isotope ratios are expressed in the standard (δ) notation in per mil (‰) relative to the international Vienna Pee Dee Belemnite (V-PDB) isotope standard. The $\delta^{13}C$ values were characterized by an average standard deviation of ± 0.1‰ defined by repeated analyses of standards (Natali & Bianchini, 2015; Bianchini & Natali, 2017). For the analysis of radiogenic isotopes rock powders were preliminarily leached with 2.5M HCl for 4 hours and then rinsed three times with Milli-Q water. After acid digestion, Sr, Nd and Pb were separated by cation-exchange chromatography and then isotopic ratios were determined using thermal ionization mass spectrometry (ThermoFinnigan MAT 262) at the Institute of Geothermal Sciences of the Kyoto University, with the methods described by Yoshikawa and Nakamura (1993), Miyazaki et al. (2003), Shibata and Yoshikawa (2004). The normalizing factors used to correct the isotopic fractionation of Sr, Nd and Pb were $^{86}Sr/^{88}Sr = 0.1194$, $^{146}Nd/^{144}Nd = 0.7219$ and 0.001% per atomic mass unit, respectively. The normalizing factor for Pb isotope ratios was determined by the analysis of NIST SRM981. The NIST 987, La Jolla and NIST981 standard solutions yield values of $^{87}Sr/^{86}Sr = 0.710279 \pm 28$ (2σ), $^{143}Nd/^{144}Nd = 0.511851 \pm 13$ (2σ), $^{206}Pb/^{204}Pb = 16.944 \pm 0.004$ (2σ), $^{207}Pb/^{204}Pb = 15.499 \pm 0.004$ (2σ) and $^{208}Pb/^{204}Pb = 36.721 \pm 0.010$ (2σ). K–Ar dating was performed by Activation Laboratories Ltd. (ActLabs; Ontario, Canada). For Ar analysis, an aliquot of bulk rock powder was weighed, loaded into the sample system of extraction, degassed at ca 100 °C during 2 days to remove the surface gases. Argon was extracted from a double vacuum furnace at 1700 °C and its concentration determined using isotope dilution with ^{38}Ar spike, which is introduced to the sample system prior to each extraction. The extracted gases are cleaned up in a two steps purification process. Then pure Ar is introduced into magnetic sector mass spectrometer (Reynolds type). Ar isotope ratios were corrected for mass-discrimination and then atmospheric argon was corrected assuming that ^{36}Ar is only from the air. Concentration of radiogenic ^{40}Ar was calculated by using the ^{38}Ar spike concentration. K analysis was performed by ICP.

3 Results

3.1 Petrography, major and trace element composition

The studied rocks are fine grained with textures varying between aphyric to porphyric. Phenocrysts are very altered and their nature can be recognised only in rare preserved relicts. They are represented mainly by feldspar (plagioclase and alkali feldspar; Table 1) partially replaced by epidote, sericite, calcite. Chlorite and serpentine were also observed, plausibly developed on phenocrysts of clinopyroxene and olivine. Ground mass is made of the same minerals, plus brown mica. Although the primary parageneses are difficult to be recognized, the presence of both plagioclase ($An_{76.3}$-$_{38.6}$) and alkali feldspar ($Ab_{57.1-3.5}$, $Or_{96.3-18.6}$) together with biotite (supporting information Table S1) is an important marker indicating that the relative magma was substantially mafic and potassic, i.e., features observed in many Cenozoic "orogenic" (subduction-related) volcanic rock associations of the circum-Mediterranean area (Wilson & Bianchini, 1998; Bianchini et al., 2008; Conticelli et al., 2009; Beccaluva et al., 2011; 2013; Conte et al., 2016). The observed petrographic features are totally distinct from those of the Late Cretaceous Calceranica lamprophyre and of the Cenozoic basic rocks of the Veneto Volcanic Province (VVP, also outcropping in Trentino; Beccaluva et al., 2007) that are usually fresh porphyric rocks containing olivine and clinopyroxene phenocrysts within a groundmass made of clinopyroxene, plagioclase, oxides ± amphibole. In spite of the observed alteration, confirmed by the correlation (r^2 ~ 0.9) between Loss on Ignition (LOI up to 8.52 wt%) and carbon content (up to 1.3 wt%), the major element budget of the studied dykes (Table 1) still conforms to that of basic volcanic rocks with SiO_2 varying between 52.2 and 58.5 wt%, TiO2 between 0.7 and 0.9 wt%, Al_2O_3 between 13.8 and 18.3 wt%, FeO between 7.6 and 10.6 wt%, MgO between 5.0 and 14.2 wt%, CaO between 1.8 and 6.8 wt%, Na_2O between 0.4 and 3.6 wt%, K_2O between 0.7 and 4.7 wt%, P_2O_5 between 0.1 and 0.2 wt%. More careful observation reveals that also CaO wt% is slightly biased, as roughly (r^2 ~ 0.4) correlated with LOI and C wt% clearly indicating the presence of 3 samples (TOL5a, TOL5b, TOL5c) that are comparatively more affected by post-magmatic processes. In any case, the restricted compositional range observed for an element scarcely mobile during weathering processes such as TiO_2, and the lack of clear relationships between LOI (and carbon) and major oxides (with the exception of CaO) suggest that the bulk rock major element composition (recalculated on anhydrous basis) still preserves information on the magmatic signature. MgO is inversely correlated with SiO_2, Al_2O_3, alkalis (Na_2O+K_2O), TiO_2 and P_2O_5, suggesting that the various rocks could reflect different degree of fractional crystallization of mafic minerals (mainly olivine). Notably, the Late Cretaceous Calceranica lamprophyre has a distinct composition characterized by SiO_2 between 37 and 41 wt%, TiO_2 up to 4.7 wt%, and Na_2O up to 4.2 wt% (Galassi et al., 1994). Similarly, also the Cenozoic VVP rocks (Beccaluva et al., 2007) are very different, as they are characterized by a sodic alkaline affinity.

Table 1. Bulk Rock major and trace element composition of basic dykes from Valsugana.

sample	TOL1	TOL1rep	TOL2	TOL5A	TOL5B	TOL5C	TOL7	TOL9	TOL10	TOL11	TOL12	TOL13	TOL14
rock type	SHO	SHO	SHO	SHO	CA	CA	CA	SHO	SHO	SHO	CA	SHO	SHO
SiO_2 (wt%)	50.26	50.76	51.00	49.61	54.31	48.31	49.74	55.55	56.41	55.32	56.02	53.09	54.28
TiO_2	0.76	0.76	0.74	0.63	0.61	0.59	0.69	0.87	0.85	0.87	0.86	0.89	0.90
AL_2O_3	14.88	15.00	14.67	13.32	13.05	12.63	15.52	17.49	17.34	17.57	17.41	15.39	15.44
$Fe2O_3$	8.24	8.05	7.90	7.83	7.09	7.79	13.86	7.20	7.21	7.43	6.82	7.48	7.33
MnO	0.19	0.19	0.20	0.11	0.11	0.13	0.17	0.06	0.06	0.06	0.06	0.14	0.14
MgO	10.16	9.82	9.57	12.02	9.45	12.95	11.74	5.33	4.85	5.25	5.19	7.91	7.12
CaO	4.85	4.79	5.63	5.15	5.02	6.25	1.00	2.30	1.77	2.25	3.22	3.90	3.77
Na_2O	1.77	1.87	1.72	0.35	0.76	0.54	1.90	3.26	3.42	3.14	3.59	1.68	1.86
K_2O	4.39	4.28	3.75	3.20	3.04	2.20	0.62	3.85	4.32	4.15	2.90	4.44	4.09
P_2O_5	0.12	0.12	0.12	0.09	0.09	0.08	0.13	0.23	0.22	0.23	0.23	0.17	0.17
C	0.55		0.58	1.14	1.05	1.28	0.16	0.34	0.28	0.33	0.33	0.53	0.55
LOI	4.38	4.38	4.69	7.68	6.47	8.52	4.62	3.86	3.55	3.74	3.69	4.91	4.92
Ni (ppm)	42	39	38	112	93	129	68	13	13	13	10	12	12
Co	34	31	32	34	30	40	29	16	18	16	15	20	20
Cr	250	250	238	571	478	612	425	61	65	57	52	129	131
V	208	209	207	186	151	188	198	148	149	152	144	152	151
Rb	277	279	224	173	178	128	25	223	226	221	158	173	167
Sr	390	398	410	118	225	177	178	354	287	382	510	389	422
Ba	423	434	466	307	360	234	198	661	870	864	556	533	521
Pb	4	5	6	32	15	10	9	6	7	8	9	14	9
Y	20.8		20.6	18.7	20.7	15.2	18.5	9.07	7.13	10.1	12.1	21.7	25.5
Zr	87.0		128	83.0	85.4	79.4	120	114	86.1	93.9	123	160	124
Nb	6.23		6.04	6.71	8.02	6.15	6.42	10.8	10.7	11.0	10.9	12.4	12.0
La	19.8		18.6	19.0	23.5	14.2	20.3	8.91	6.52	9.11	12.5	27.7	34.1
Ce	43.1		36.7	37.6	50.3	29.2	48.4	19.6	16.4	23.6	29.8	69.6	82.2
Pr	4.97		4.77	4.70	5.73	3.79	5.63	2.76	2.04	3.07	3.76	7.80	8.94
Nd	19.7		19.1	18.5	22.1	15.2	23.1	11.5	8.67	13.1	15.4	31.1	35.0
Sm	4.23		4.13	3.93	4.54	3.31	5.01	2.53	1.95	2.95	3.33	6.25	7.00
Eu	0.87		0.94	0.94	0.98	0.85	1.21	0.79	0.64	0.93	0.89	1.50	1.63
Gd	4.29		4.16	3.95	4.50	3.24	4.65	2.37	1.89	2.77	3.09	5.71	6.47
Tb	0.74		0.72	0.68	0.76	0.57	0.77	0.42	0.33	0.50	0.55	0.94	1.05
Dy	3.64		3.65	3.34	3.70	2.86	3.56	2.11	1.73	2.54	2.74	4.52	4.95
Ho	0.81		0.83	0.74	0.81	0.64	0.77	0.47	0.40	0.57	0.61	0.98	1.06
Er	2.12		2.16	1.95	2.11	1.68	2.00	1.25	1.08	1.49	1.59	2.55	2.77
Tm	0.38		0.40	0.36	0.39	0.31	0.37	0.23	0.20	0.27	0.29	0.46	0.50
Yb	2.02		2.14	1.91	2.08	1.68	2.01	1.26	1.07	1.47	1.57	2.49	2.61
Lu	0.33		0.36	0.32	0.34	0.28	0.34	0.21	0.17	0.23	0.26	0.40	0.42
Hf	2.60		3.18	2.65	2.83	2.57	3.34	2.93	2.73	2.95	3.10	4.03	3.95
Ta	0.29		0.28	0.35	0.44	0.32	0.33	0.49	0.48	0.50	0.49	0.60	0.59
Th	6.08		6.63	7.02	9.71	6.07	7.87	6.47	6.27	8.70	7.74	13.2	13.4
U	0.93		0.94	1.45	2.06	1.32	1.51	1.27	1.46	1.58	1.23	2.20	2.20

Note: SHO = shoshonite series; CA = calcalkaline series

Plotted in the Total Alkali Silica (TAS) diagram, the studied dykes include subalkaline and transitional products, which according to the K_2O vs SiO_2 diagram (Fig. 2) pertain to the calcalkaline and shoshonite series, respectively. In particular, shoshonite products seem to prevail (8 samples out of 12). These variations conform to those of magma series typically occurring in convergent plate margins in connection with the occurrence of subduction processes (e.g.: Bianchini et al., 2008; Conticelli et al., 2009; Mattioli et al., 2012; Beccaluva et al., 2013 and references therein). On the basis of the major element chemistry, Valsugana dykes could be in principle related to the Oligo-Miocene magmatic episode that generated the Adamello pluton. However, the subordinate mafic rocks outcropping in the Adamello complex are calcalkaline, while the shoshonite affinity is not recorded (Alagna et al., 2010). Analogously, also the older basic rocks observed as enclaves in the Permian granites of the Cima D’Asta complex (Rottura et al., 1998) are calcalkaline, and in this view, best analogues of the Valsugana dykes in the Trentino region are represented by the basic magmatic rocks erupted during the Trias (Ladinic) in the Dolomites (Sloman 1989; Bonadiman et al., 1994; Casetta et al., 2017).

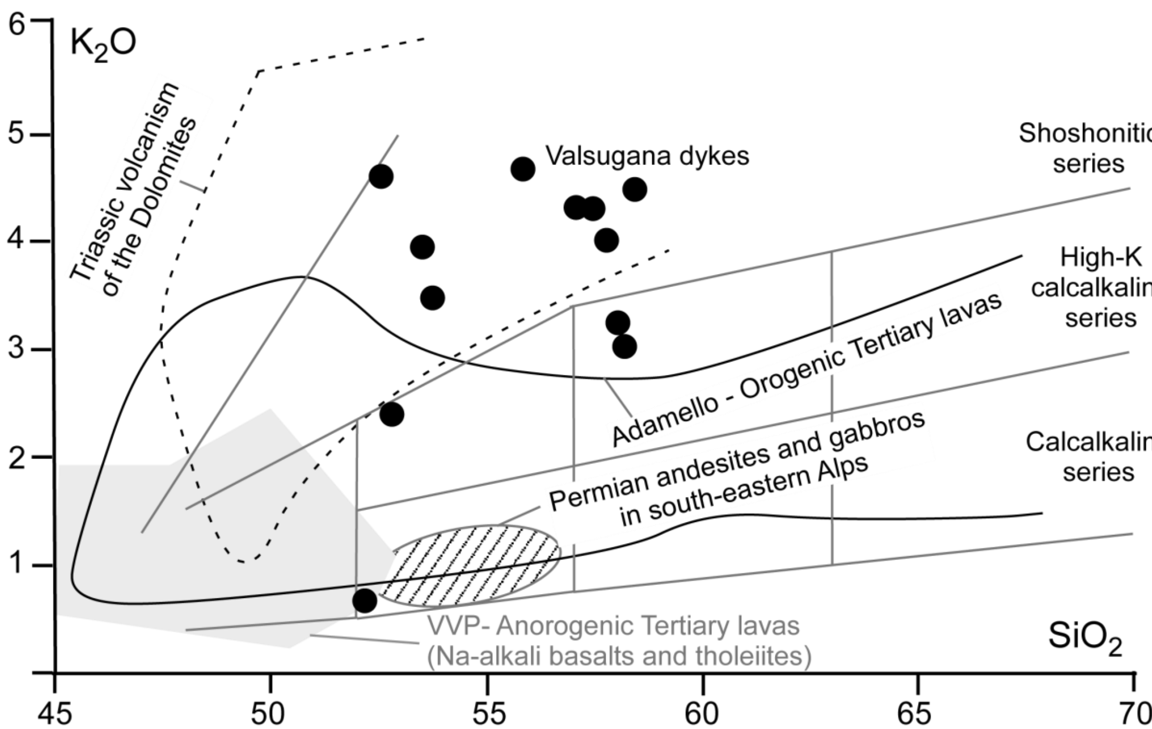

Figure 2. K_2O vs SiO_2 classification diagram reporting compositions (black dots) of the studied Valsugana basic dykes. Compositions of other rocks from neighbouring magmatic occurrences such as Calceranica lamprophyre (Galassi et al., 1994), Tertiary anorogenic lavas (Na-alkaline basalts and tholeiites) of the Veneto Volcanic Province (VVP; Beccaluva et al., 2007), Tertiary calcalkaline mafic rocks from Adamello (Alagna et al., 2010), Triassic shoshonite rocks from the Dolomites (Authors unpublished data), Permian high-K calcalkaline basalts and gabbros (Rottura et al., 1998) are reported for comparison..

The incompatible trace element distribution (Table 1) highlighted by mantle normalized spiderdiagrams (Fig. 3) show for all sample comparable order of concentration, irrespective of the extent of alteration. In particular, all samples invariably display negative anomalies in High Field Strength Elements (HFSE) such as Ti, Nb, Ta typical of subduction related magmas. They are different from both the Calceranica lamprophyre and the basic rocks of the VVP that have positive anomalies in HFSE, and recall features that are intermediate between the basic rocks associated to the Permian granitoids outcropping in Valsugana (Cima d'Asta Complex) and to the Triassic shoshonite volcanics outcropping in the Dolomites.

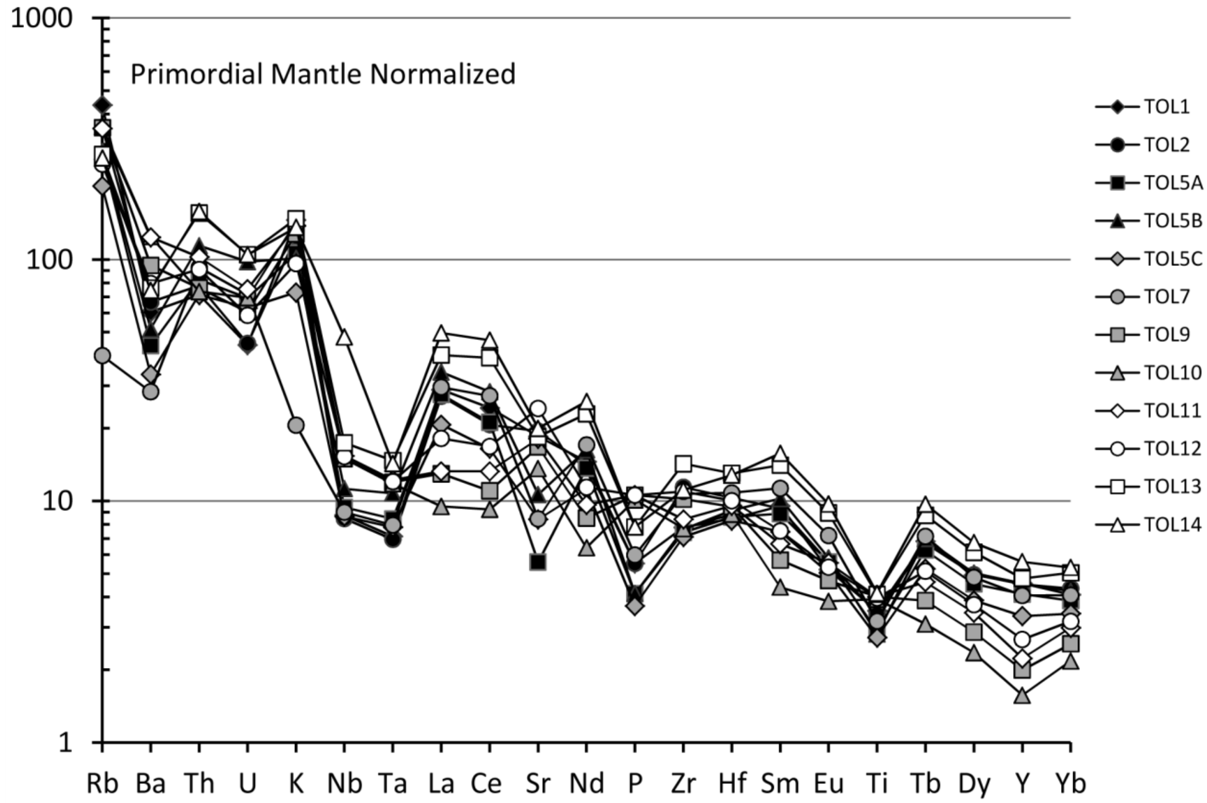

Figure 3. Primordial mantle normalized spiderdiagrams showing the incompatible element distribution of the studied Valsugana basic dykes. Normalization coefficients from Sun and McDonough (1989).

Coherently, in the Ce/Yb vs Ta/Yb and Th/Yb vs Ta/Yb diagrams (Fig. 4) proposed by Pearce et al. (1982) Valsugana dykes plot at the boundary between the calcalkaline and the shoshonite fields.

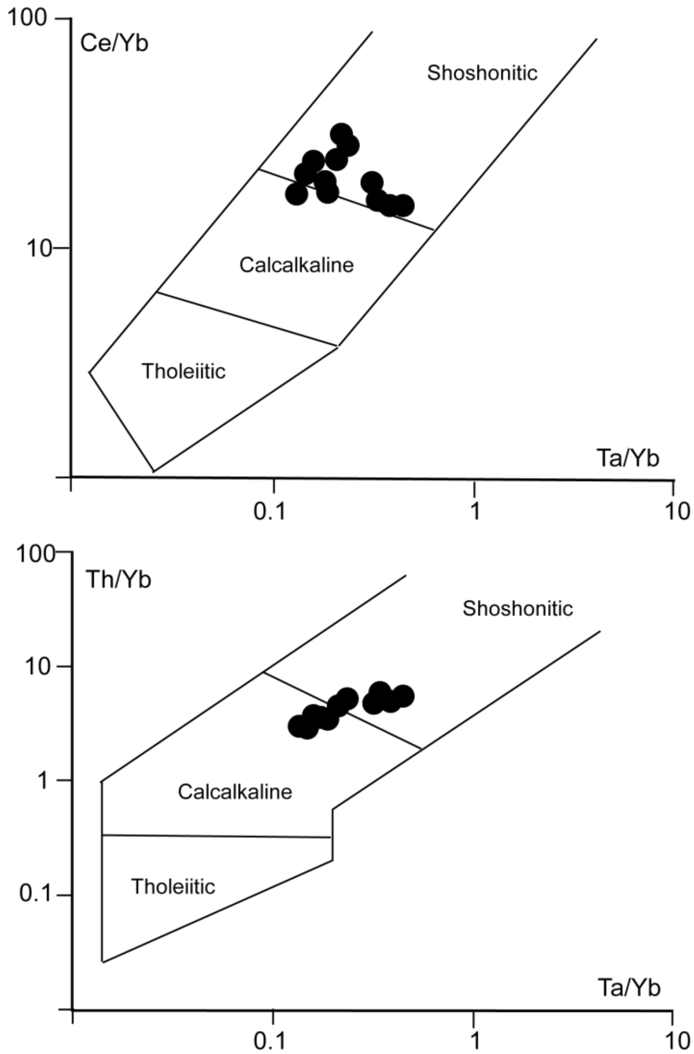

Figure 4. Composition of basic dykes from Valsugana (black dots) plotted in Ta/Yb-Ce/Yb and Ta/Yb-Th/Yb diagrams reporting discriminative fields between tholeiitic, calcalkaline and shoshonitic suites (taken from Pearce, 1982).

This affinity, certainly attributable to a convergent plate setting and intermediate between the calcalkaline and shoshonite series, is confirmed by the use of recent tectonomagmatic diagrams (Fig. 5) such as those proposed by Hastie et al. (2007) and Saccani (2015).

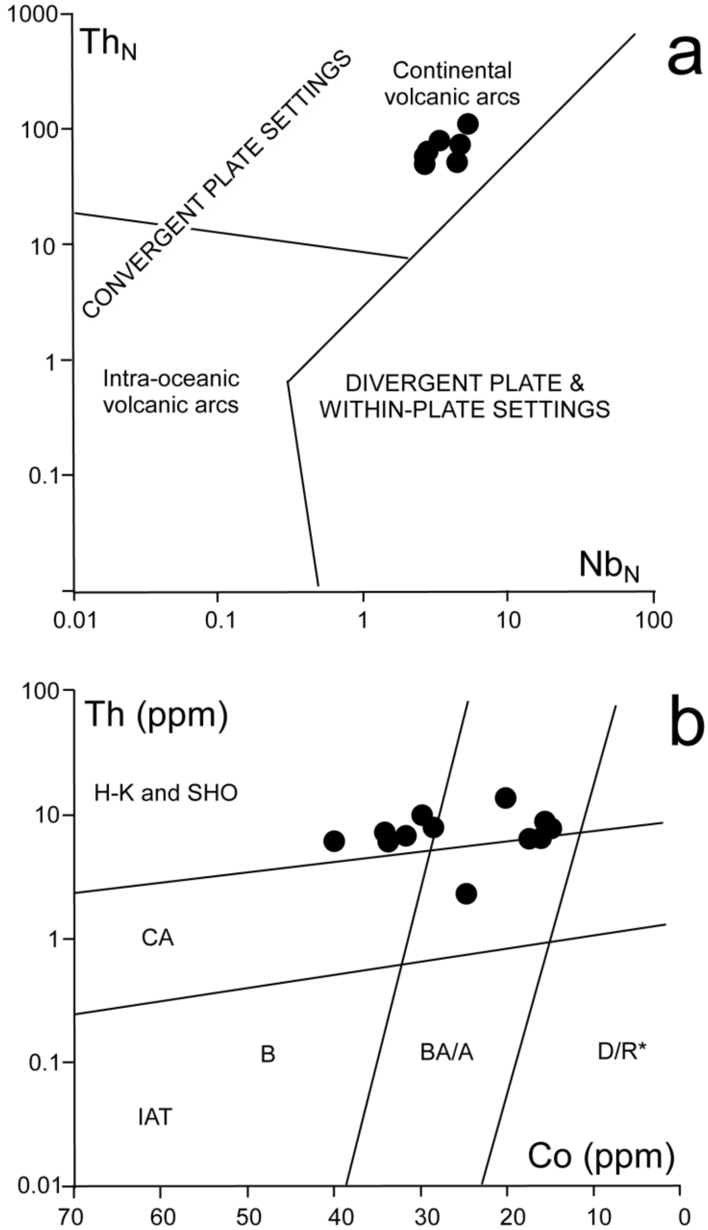

Figure 5. Composition of the studied basic dykes from Valsugana (black dots) plotted in: a) N-MORB (Sun & McDonough, 1989) normalized Th_N vs. Nb_N tectono-magmatic discrimination diagram proposed by Saccani (2015); b) Th vs. Co discrimination diagram for convergent margins magmatic rocks (Hastie et al., 2007).

3.2 $\delta^{13}C$ and Sr-Nd-Pb isotopic composition

The $\delta^{13}C$ and Sr-Nd-Pb isotopic compositions, reported in Table 2, show the following ranges: $\delta^{13}C$ from -9.9 to -12.5‰, $^{87}Sr/^{86}Sr$ 0.7093-0.7464, $^{143}Nd/^{144}Nd$ 0.5123-0.5121, $^{206}Pb/^{204}Pb$ 18.5-19.6, $^{207}Pb/^{204}Pb$ 15.6-15.7, $^{208}Pb/^{204}Pb$ 38.6-40.5. Isotopic data of the Valsugana dykes have to be properly "filtered" to distinguish the magmatic signature from isotopic variation induced by post-magmatic processes.

Table 2. C-Sr-Nd-Pb isotopic composition of basic dykes from Valsugana.

	$\delta^{13}C$ (‰)	$^{87}Sr/^{86}Sr$	$^{143}Nd/^{144}Nd$	$^{206}Pb/^{204}Pb$	$^{207}Pb/^{204}Pb$	$^{208}Pb/^{204}Pb$
TOL1	-12.5	0.725234	0.512106	19.571	15.724	40.497
TOL2	-10.3	0.723042	0.512208	19.439	15.741	40.141
TOL5A	-9.9	0.746408	0.512277	18.546	15.652	38.671
TOL5B	-11.3					
TOL5C	-10.2	0.725437	0.512257	18.801	15.652	38.901
TOL7	-11.8	0.709257	0.512215	19.365	15.699	39.412
TOL9	-10.9	0.716827	0.512147	19.328	15.689	39.559
TOL10	-12.0					
TOL11	-11.3	0.716640	0.512161	19.019	15.680	39.226
TOL12	-11.8	0.714118	0.512141	19.261	15.682	39.456
TOL13	-10.2	0.714894	0.512200	19.094	15.708	39.291
TOL14	-10.9	0.714770	0.512164	19.142	15.691	39.279

Carbon and LOI are inversely correlated with the $\delta^{13}C$, and the more altered samples are characterized by $\delta^{13}C$~ -9.9‰, whereas relatively unaltered samples display $\delta^{13}C$ ~ -12.5‰. While the latter is compatible with carbon isotopic composition of magmatic rocks in convergent settings (Bianchini & Natali, 2017), the trend toward less negative isotopic ratios is plausibly reflecting the interaction with deuteric components (e.g., Djouka-Fonkwé et al., 2012).

The Sr isotopic composition is correlated with the Rb/Sr elemental ratio (Fig. 6a), but totally decoupled from the other isotopic systematics. The Rb/Sr vs $^{87}Sr/^{86}Sr$ relationship gives a regression line having correlation coefficient r^2 of 0.94, that could be interpreted as a mixing between a deep magmatic end-member and components acquired during (and after) the dykes emplacement. This is confirmed by the compositions of the local host rocks of the basement that extend along the same trend toward higher Rb/Sr and $^{87}Sr/^{86}Sr$ values. It is interesting to note that the less radiogenic Sr composition is referred to the sample TOL 7 ($^{87}Sr/^{86}Sr$ 0.7093), which is characterized by relatively high MgO (i.e., an undifferentiated magma composition) and low LOI. $^{143}Nd/^{144}Nd$ appears correlated with LOI, C content and $\delta^{13}C$ (r^2 ~ 0.6), and samples scarcely affected by post-magmatic processes display isotopic composition ~ 0.5122.

Comparison with the isotopic fingerprint of other magmatic rocks of neighbouring occurrences can be done mainly on the basis of $^{87}Sr/^{86}Sr$ and $^{143}Nd/^{144}Nd$ that are available in the literature (Fig. 6b). The data of the Valsugana dykes presented in this study are totally distinct from those characteristics of the Late Cretaceous Calceranica Lamprophyre and those of the VVP volcanic rocks (Beccaluva et al., 2007). The less radiogenic $^{87}Sr/^{86}Sr$, if corrected for the estimated age of these dykes (the average of the two K-Ar ages reported in the next section) correspond to a $^{87}Sr/^{86}Sr_{initial}$ of 0.7076 that is coupled with a $^{143}Nd/^{144}Nd_{initial}$ of 0.5120. These values trend toward the isotopic ranges recorded in the Triassic calcalkaline/shoshonitic magmatic rocks outcropping in the Dolomites (Bonadiman et al., 1994; Marrocchino et al., 2002; Casetta et al., 2016) and those of mafic lithologies that are associated with the Permian granitoids (Rottura et al., 1998). These values diverge from the notional mantle array and are rarely recorded in anorogenic magmatic occurrences. In fact, very radiogenic Sr isotopic compositions and very unradiogenic Nd isotopic compositions better conform to those of magmas of subduction related settings, especially in collisional zones where there is chance of recycling of crustal components in the mantle (Bianchini et al., 2008. Conticelli et al., 2007; 2009; Bianchini et al., 2015).

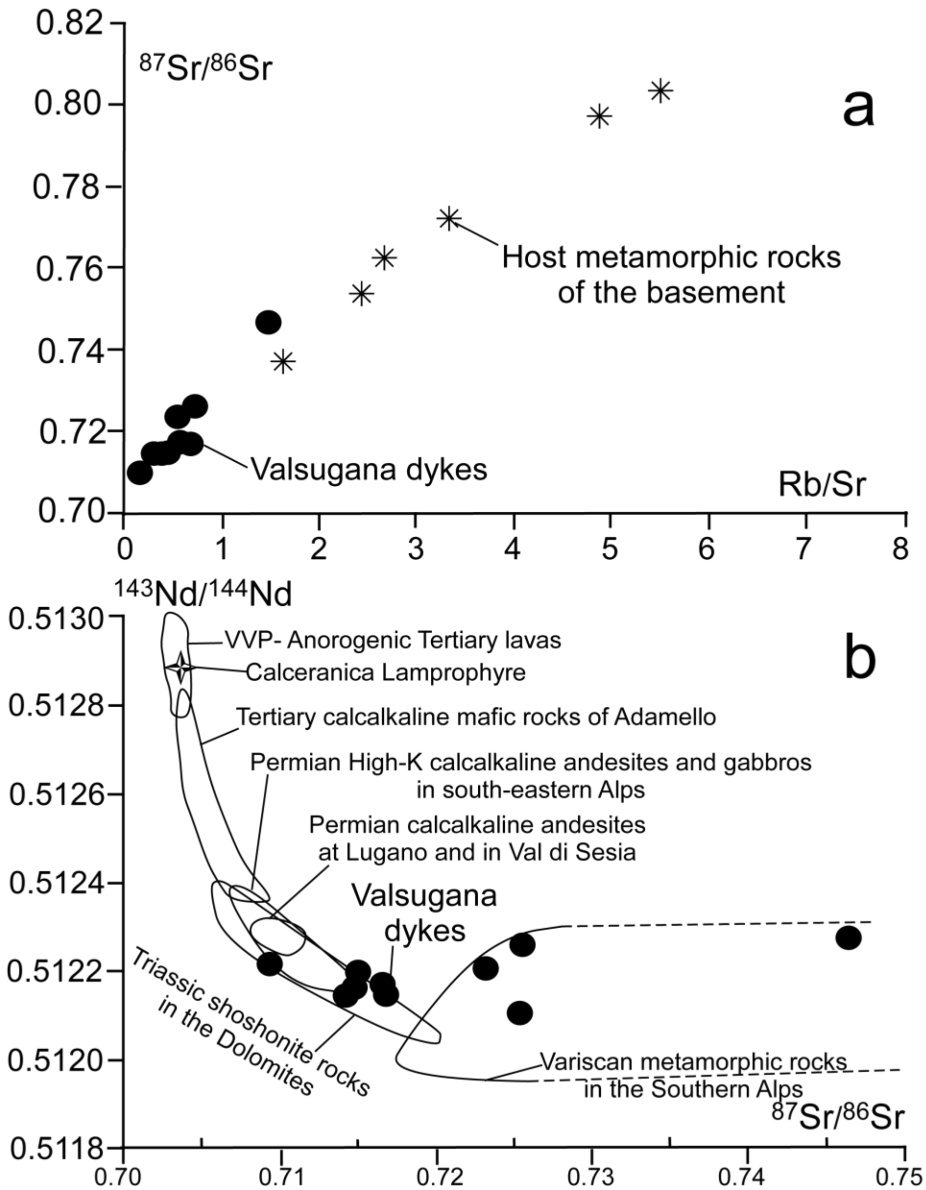

Figure 6. ^{87}Sr/^{86}Sr vs Rb/Sr diagram, in which the studied dykes from Valsugana (black dots) are compared with the host metamorphic rocks from the basement collected exactly in the same area (Meli & Sassi, 2004); b) ^{143}Nd/^{144}Nd vs ^{87}Sr/^{86}Sr diagram in which the studied dykes from Valsugana are compared with the neighbouring magmatic occurrences such as the Calceranica lamprophyre and the Tertiary anorogenic lavas (Na-alkaline basalts and tholeiites) of the Veneto Volcanic Province (VVP; Beccaluva et al., 2007), the Tertiary calcalkaline mafic rocks from Adamello (Kagami et al., 1991; Alagna et al., 2010), Triassic shoshonite rocks from the Dolomites (Bonadiman et al., 1994), Permian high-K calcalkaline basalts and gabbros (Macera et al., 1994; Rottura et al., 1998) and Permian andesites from Lugano and Val di Sesia (Sinigoi et al., 2016); since Nd isotopic values are not available for the metamorphic rocks of the studied area, isotopic values of the basement are referred to a neighbouring sector of the South-Alpine region characterized by similar micashists and paragneisses (Pinarelli et al., 2008).

As concerns the lead isotopic composition, the studied dykes show isotopic values particularly radiogenic ($^{206}Pb/^{204}Pb$ up to 19.57, $^{207}Pb/^{204}Pb$ up to 15.74, $^{208}Pb/^{204}Pb$ up to 40.49) compared with literature data available for Cenozoic, Permian and Triassic volcanics on neighbouring occurrences. This evidence could recall what observed in suites of volcanic rocks affected by weathering and differential element mobilization (Marschik et al., 2003), possibly indicating a long term history in which Pb has been preferentially leached leaving high U/Pb and Th/Pb residua that ultimately led to radiogenic Pb compositions. However, the good correlations observed in the $^{206}Pb/^{204}Pb$ vs $^{208}Pb/^{204}Pb$ and $^{206}Pb/^{204}Pb$ vs $^{207}Pb/^{204}Pb$ diagrams (Fig. 7) do not conform with scattered variations that are often induced by crustal contamination during magma emplacement or to late-stage deuteric alteration. In this view, the systematic Pb isotopic differences respect to volcanic products of neighbouring occurrences can be interpreted assuming that the Valsugana basic dykes reflect an independent volcanic phase having distinctive magma sources.

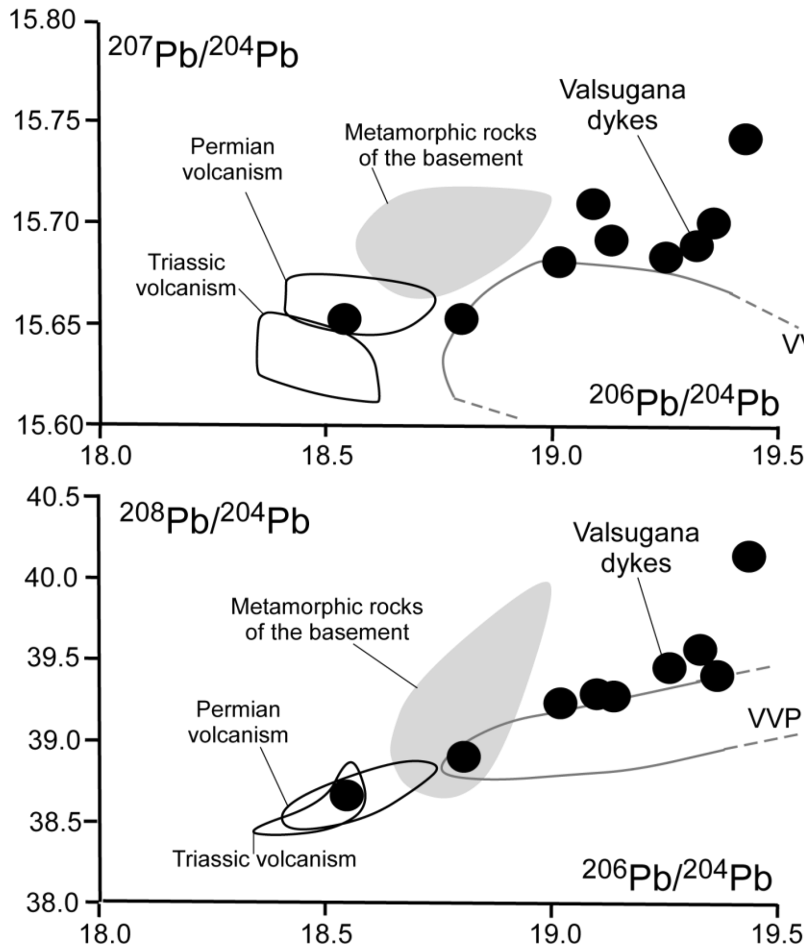

Figure 6. Lead isotopic composition of the studied basic dykes from Valsugana (black dots). Compositions of other rocks from neighbouring magmatic occurrences (Nimis et al., 2012 and references therein) and that of the South-Alpine basement (Pinarelli et al., 2008) are reported for comparison.

3.3 K-Ar datings

The preliminary K-Ar dating was carried out on two samples, characterized by lack of pervasive alteration, selecting chips at the microscope before powdering. Notably, these samples, plotted in a K_2O vs LOI diagram are representative of the sample population. Dating yield ages of 236±6 for TOL13 and 251±7 Ma for TOL1, suggesting the existence in Valsugana of a previously unknown magmatic episode generating basic magmas in a time window intermediate between that of neighbouring, well represented volcanic phases, such as the extensive ignimbrite eruptions of the Athesian platform (around 280-270 Ma; D'Amico et al., 1980; D'Amico & Del Moro, 1988; Marocchi et al., 2008) and that occurred in Dolomites mainly at Predazzo-Monzoni (around 237-230 Ma; Laurenzi et al., 1994).

A tectono-magmatic episode of this age could explain 1) the reopening of the Rb-Sr system recorded at ca. 240 Ma in the Athesian volcanic products (D'Amico et al., 1980; D'Amico & Del Moro, 1988) and 2) the hydrothermal processes ultimately leading to the formation of ore deposits in carbonate rocks of the Werfen formation in the studied area (Nimis et al., 2012 and references therein) and in neighbouring sectors of the southern Alps (Martin et al., 2017).

4 Conclusive remarks

In spite of postmagmatic processes that potentially altered the original features, the petrographic evidences, major element compositions, trace element distribution and isotopic signatures of the studied dykes from Valsugana still provide valuable petrological information, allowing comparison with modern volcanic counterparts. Considering the observed spatial location, the timing inferred from K-Ar datings (236±6 and 251±7 Ma), and the geochemical signature, we propose that the studied dykes represent a transition between the Permian and the Triassic volcanism that are known in neighbouring sectors of the Southern Alps, following the end of the Variscan orogenic cycle. On the other hand, a possible relation between these dykes and the Cenozoic (Alpine) tectono-magmatic phases (an hypothesis proposed in the notes of the geological map of Trento) seems to be totally unwarranted.

In this view, the investigated Early Triassic dykes would represent additional evidence of post-collisional magmatism that has been recognised in the South-Alpine domain in Trentino (Casetta et al., 2017) but also westward in Lombardia (Crisci et al., 1984; Cassinis et al., 2008; Armienti et al., 2003; Beltrán-Triviño et al., 2016) and in the Ivrea-Verbano zone (Mazzucchelli et al., 2010; Sinigoi et al., 2016), and eastward in Veneto (Bellieni et al., 2010; Testa et al., 2013).

Different hypotheses have been proposed to explain the occurrence of Permo-Triassic subduction related magmatic rocks in the South-Alpine domain. Some Authors are tentatively proposing the persistence of an active Permo-Triassic subduction, whereas others ascribe the metasomatism of the mantle sources to the Variscan cycle, proposing that partial melting and magma genesis were delayed respect to the time of subduction processes (Beltrán-Triviño et al., 2016 and references therein).

Classic reconstructions (Stampfli, 2005; Kroner & Romer, 2013) consider the Variscan orogen as the result of subduction of several oceanic domains interposed between Gondwana and Laurussia during Devonian and Carboniferous, with subsequent continental collision(s) that structured most of the Variscides, also indicating that active subduction of the Palaeotethys was still active at 280-250 Ma, dipping toward a continental margin including the south-Alpine region (Bonin, 1998; Spiess et al., 2010). Recent studies (Franke et al., 2017) put more emphasis on the role of microplates/blocks sandwiched between Gondwana and Laurussia. They suggest that parts of south-eastern Europe, including the South-Alpine domain, were formed by the break-up of the

northern Gondwana margin from the Late Cambrian onwards, in connection with important transtensional movements, leaving rifted continental basins or narrow oceanic seaways, similar to those sutured during the Alpine orogenic cycle.
In our view, the subduction processes that induced metasomatism in mantle sources of the South-Alpine region occurred in connection with the Carboniferous (-Permian?) consumption of the lithosphere of rifted continental basins and narrow oceanic domains. Diachronous subductions dipped beneath continental blocks interposed between the major plates (Giacomini et al., 2006; Dallagiovanna et al., 2009) with a geodynamic style that anticipated that observed in the Central Mediterranean during the subsequent Cenozoic (Alpine) orogenic cycle. The delineated framework is compatible with the pervasive recycling of continental crust components within the mantle wedge, as widely observed in the magma genesis of Cenozoic volcanic occurrences throughout the Mediterranean region (Bonin, 2004; Bianchini et al., 2008; 2011; 2015; Avanzinelli et al., 2009; Beccaluva et al., 2011; 2013; Conticelli et al., 2007; 2009). In summary, our favoured hypothesis is compatible with the tectono-magmatic model of Schuster and Stüwe (2008) that relates the observed magmatism, typically including shoshonite products, to the extensional tectonics that occurred in the area in a post-collisional setting that followed the Variscan orogenic cycle.

In any case, the vestiges of Permo-Triassic volcanic events aligned along a 300 km E-W belt in the South Alpine region indicate the existence of tectonic structures that were effective at least since the Variscan tectono-magmatic phase, well before the Alpine cycle. In order to constrain the discussed hypotheses, future investigations need to discover further outcrops characterized by preserved magmatic parageneses and to carry out more accurate and precise datings.

Acknowledgments, Samples, and Data

Additional data are available in the supporting information. Andrea Risplendente is acknowledged for his help during EMPA measurements, Renzo Tassinari for the XRF and ICP-MS analysis, and Massimo Tiepolo for the constructive discussion of the obtained data.

References

Alagna, K.E., Peccerillo, A., & Martin, S. (2010). Tertiary to Present evolution of orogenic magmatism in Italy. *Journal of Virtual Explorer*, 36, paper 18.

Armienti, P., Corazzato, C., Groppelli, G., Natoli, E., & Pasquarè, G. (2003). Geological and petrographical study of Montecampione Triassic subvolcanic bodies (Southern Alps, Italy): Preliminary geodynamic results. *Bollettino della Società Geologica Italiana*, 2, 67–78.

Avanzinelli, R., Lustrino, M., Mattei, M., Melluso, L., & Conticelli S. (2009). Potassic and ultrapotassic magmatism in the circum-Tyrrhenian region: Significance of carbonated pelitic vs. pelitic sediment recycling at destructive plate margins. *Lithos*, 113, 213-227.

Beccaluva, L., Bianchini, G., Bonadiman, C., Coltorti, M., Milani, L., Salvini, L., … Tassinari, R. (2007). Intraplate lithospheric and sublithospheric components in the Adriatic domain: nephelinite to tholeiite magma generation in the Paleogene Veneto Volcanic Province, Southern Alps. *Geological Society of America Special Paper*, 418, 131-152.

Beccaluva, L., Bianchini, G., Natali, C., Siena, F. (2011). Geodynamic control on orogenic and anorogenic magmatic phases in Sardinia and Southern Spain: Inferences for the Cenozoic evolution of the western Mediterranean. *Lithos*, 123, 218-224.

Beccaluva, L., Bianchini, G., Mameli, P., & Natali C. (2013). Miocene shoshonite volcanism in Sardinia: Implications for magma sources and geodynamic evolution of the central-western Mediterranean. *Lithos*, 180-181, 128-137.

Bellieni, G., Fioretti, A.M., Marzoli, A., & Visonà D. (2010). Permo–Paleogene magmatism in the eastern Alps. *Rendiconti Lincei*, 21, 51–71.

Beltrán-Triviño, A., Winkler, W., von Quadt, A., & Gallhofer, D. (2016). Triassic magmatism on the transition from Variscan to Alpine cycles: evidence from U–Pb, Hf, and geochemistry of detrital minerals. Swiss Journal of Geosciences, 109, 309–328.

Bianchini, G., Beccaluva, L., & Siena, F. (2008). Post-collisional and intraplate Cenozoic volcanism in the rifted Apennines/Adriatic domain. *Lithos*, 101, 125-140.

Bianchini, G., Beccaluva, L., Nowell, G.M., Pearson, D.G., & Siena, F. (2011). Mantle xenoliths from Tallante (Betic Cordillera): insights into the multi-stage evolution of the south Iberian lithosphere. *Lithos*, 124, 308-318.

Bianchini, G., Braga, R., Langone, A., Natali, C., & Tiepolo, M. (2015). Metasedimentary and igneous xenoliths from Tallante (Betic Cordillera, Spain): Inferences on crust–mantle interactions and clues for post-collisional volcanism magma sources. *Lithos*, 220-223, 191-199.

Bianchini, G., & Natali, C. (2017). Carbon elemental and isotopic composition in mantle xenoliths from Spain: Insights on sources and petrogenetic processes. *Lithos*, 272, 84-91.

Bonadiman, C., Coltorti, M., & Siena, F. (1994). Petrogenesis and T-fO2 estimates of Mt. Monzoni complex (Central Dolomites, Southern Alps): a Triassic shoshonitic intrusion in a transcurrent geodynamic setting. *European Journal of Mineralogy*, 6, 943-966.

Bonin, B. (1998). Orogenic to non-orogenic magmatic events: overview of the Late Variscan magmatic evolution of the Alpine belt. *Turkish Journal of Earth Sciences*, 7, 133-143.

Bonin, B. (2004). Do coeval mafic and felsic magmas in post-collisional to within-plate regimes necessarily imply two contrasting, mantle and crustal, sources? A review. *Lithos*, 78, 1-24

Casetta, F., Coltorti, M., Marrocchino, E., & Bonadiman, C. (2016). A shoshonitic multi-pulse intrusion in the Southern Alps domain (NE Italy): the Predazzo Intrusive Complex (PIC). *Rendiconti Online della Società Geologica Italiana*, Suppl. n. 1, 40, 223.

Casetta, F., Coltorti, M., & Marrocchino, E. (2017). Petrological evolution of the Middle Triassic Predazzo Intrusive Complex, Italian Alps. *International Geology Review*, doi.org/10.1080/00206814.2017.1363676.

Cassinis, G., Cortesogno, L., Gaggero, L., Perotti, C.R., & Buzzi, L. (2008). Permian to Triassic geodynamic evolution of the Brescian Prealps (eastern Lombardy, Italy). *Italian Journal of Geosciences*, 127, 501-518.

Conte, A.M., Perinelli, C., Bianchini, G., Natali, C., Martorelli, E., & Chiocci, F.L. (2016). New insights on the petrology of submarine volcanics from the Western Pontine Archipelago (Tyrrhenian Sea, Italy). *Journal of Volcanology and Geothermal Resources*, 327, 223-239.

Conticelli, S., Carlson, R.W., Widom, E., & Serri, G. (2007). Chemical and isotopic composition (Os, Pb, Nd and Sr) of Neogene to Quaternary calc-alkalic, shoshonitic, and ultrapotassic mafic rocks from the Italian peninsula: Inferences on their mantle sources. *Geological Society of America Special Paper*, 418, 171-202.

Conticelli, S., Guarnieri, L., Farinelli, A., Avanzinelli, R., Mattei, M., Bianchini, G., … Venturelli G. (2009). Trace elements and Sr-Nd-Pb isotopes of K-rich, shoshonitic, and calcalkaline magmatism of the Western Mediterranean Region: genesis of ultrapotassic to calc-alkaline magmatic associations in a post-collisional geodynamic setting. *Lithos*, 107, 68-92.

Crisci, C.M., Ferrara, G., Mazzuoli, R., & Rossi, P.M. (1984). Geochemical and geochronological data on Triassic volcanism of the Southern Alps of Lombardy (Italy): genetic implications. *Geologische Rundschau*, 73, 293–306.

Dallagiovanna, G., Gaggero, L., Maino, M., Seno, S., & Tiepolo, M. (2009). U-Pb zircon ages for post-Variscan volcanism in the Ligurian Alps (Northern Italy). *Journal of the Geological Society*, 166, 101-114.

D'Amico, C., Del Moro, A., Freddo, A., & Pardini, G. (1980). Studio radiometrico delle ignimbriti riolitiche atesine, gruppo superiore. *Rendiconti della Società Italiana di Mineralogia e Petrologia*, 36, 703-716.

D'Amico, C., & Del Moro, A. (1988). Permian and Triassic Rb-Sr dating in the Permian rhyodacitic ignimbrites of Trentino (Southern Alps). *Rendiconti della Società Italiana di Mineralogia e Petrologia*, 43, 171-180.

Djouka-Fonkwé, M.L., Kyser, K., Clark, A.H., Urqueta, E., Oates, C.J., & Ihlenfeld, G. (2012). Recognizing Propylitic Alteration Associated with Porphyry Cu-Mo Deposits in Lower Greenschist Facies Metamorphic Terrain of the Collahuasi District, Northern Chile-Implications of Petrographic and Carbon Isotope Relationships. *Economic Geology*, 107, 1457-1478.

Franke, W., Cocks, L.R.M., & Torsvik, T.H. (2017). The Palaeozoic Variscan oceans revisited. *Gondwana Research*, 48, 257-284

Galassi, B., Monese, A., Ogniben, G., Siena, F., & Vaccaro, C. (1994). Age and nature of lamprophyric dykes at Calceranica (Trento). *Mineralogica et Petrographica Acta*, 37, 163-171.

Giacomini, F., Bomparola, R.M., Ghezzo, C., & Guldbransen, H. (2006). The geodynamic evolution of the Southern European Variscides: constraints from the U/Pb geochronology and geochemistry of the lower Palaeozoic magmatic-sedimentary sequences of Sardinia (Italy). *Contribution to Mineralogy and Petrology*, 152, 19-42.

Hastie, A.R., Kerr, A.C., Pearce, J.A., & Mitchell, S.F. (2007). Classification of altered volcanic island arc rocks using immobile trace elements: development of the Th-Co discrimination diagram. *Journal of Petrology*, 48, 2341-2357.

Kagami, H., Ulmer, P., Hansmann, W., Dietrich, V., & Steiger, H. (1991). Nd-Sr isotopic and geochemical characteristics of the southern Adamello (Northern Italy) intrusives: implications for crustal versus mantle origin. *Journal of Geophysical Research*, 96, 14331-14346.

Kroner, U., & Romer, R.L. (2013). Two plates — Many subduction zones: The Variscan orogeny reconsidered. *Gondwana Research*, 24, 298–329.

Laurenzi, M., Visonà, D., & Zantedeschi, C. (1994). High resolution Ar/Ar chronology of Predazzo Magmatic complex (Southern Alps, Italy), p.186. Abstracts of the eight international conference on geochronology, cosmochronology, and isotope geology. Berkley, California, USA (June 5-11, 1994).

Macera, P., Del Moro, A., Bargossi, G.M., Campana, R., & Rottura, A. (1994). Polygenetic nature of the Cima d'Asta intrusive complex, Southern Alps, Italy. Inferences from petrological, geochemical and isotopic (Sr and Nd) data. *Lithos*, 32, 47-62

Marocchi, M., Morelli, C., Mair, V., Klötzli, U., & Bargossi, G.M. (2008). Evolution of Large Silicic Magma Systems: New U-Pb Zircon Data on the NW Permian Athesian Volcanic Group (Southern Alps, Italy). *Journal of Geology*, 116, 480–498.

Marrocchino, E., Coltorti, M., Visonà, D., & Thirwall, M.F. (2002). Petrology of Predazzo magmatic complex (Trento, Italy). *Goldschmidt Conference Abstract 2002*, A486.

Marschik, R., Chiaradia, M., & Fontbote, L. (2003). Implications of Pb isotope signatures of rocks and iron oxide Cu-Au oresin the Candelaria-Punta del Cobre district, Chile. *Mineralium Deposita*, 38, 900–912.

Martin, S., Toffolo, L., Moroni, M., Montorfano, C., Secco, L., Agnini, C., Nimis, P., & Tumiati, S. (2017). Siderite deposits in northern Italy: Early Permian to Early Triassic hydrothermalism in the Southern Alps. *Lithos*, 284-285, 276-295.

Mattioli, M., Lustrino, M., Ronca, S., & Bianchini, G. (2012). Alpine subduction imprint in Apennine volcaniclastic rocks. Geochemical–petrographic constraints and geodynamic implications from Early Oligocene Aveto-Petrignacola Formation (N Italy). *Lithos*, 134–135, 201-220.

Mazzucchelli, M., Zanetti, A., Rivalenti, G., Vannucci, R., Teixeira Correia, C., & Celso Gaeta Tassinari, C. (2010). Age and geochemistry of mantle peridotites and diorite dykes from the Baldissero body: Insights into the Paleozoic–Mesozoic evolution of the Southern Alps. *Lithos*, 119, 485–500.

Meli, S., & Sassi, F.P. (2004). Rb-Sr and $^{40}Ar/^{39}Ar$ age constraints on the Variscan metamorphism recorded by Ordovician acidic metavolcanic rocks in the Eastern Southalpine basement. *Rendiconti Lincei*, 15, 205-223.

Miyazaki, T., Shibata, T., & Yoshikawa, M. (2003). New synthesis method of silica-gel for Lead isotope analysis. *Proceedings of the Japan Academy*, 79B, 58–62.

Natali, C., & Bianchini, G. (2015). Thermally based isotopic speciation of carbon in complex matrices: a tool for environmental investigation. *Environmental Science and Pollution Researches*, 22, 12162-12173.

Nimis, P., Omenetto, P.,Giunti, I., Artioli, G., & Angelini, I. (2012). Lead isotope systematics in hydrothermal sulphide deposits from the central-eastern Southalpine (northern Italy). *European Journal of Mineralogy*, 24, 23–37.

Pearce, J.A. (1982). Trace element characteristics of lavas from destructive plate boundaries. In: Thorpe, R.S. (ed), Andesites: Orogenic Andesites and Related Rocks. John Wiley & Sons, Chichester, 525 –548.

Pinarelli, L., Bergomi, M.A., Boriani, A., & Giobbi, E. (2008). Pre-metamorphic melt infiltration in metasediments: Geochemical, isotopic (Sr, Nd, and Pb), and field evidence from Serie dei Laghi (Southern Alps, Italy). *Mineralogy and Petrology*, 93, 213-242.

Rottura, A., Bargossi, G.M., Caggianelli, A., Del Moro, A., Visonà D., & Tranne, C.A. (1998). Origin and significance of the Permian high-K calc-alkaline magmatism in the central-eastern Southern Alps, Italy. *Lithos*, 45, 329-348.

Saccani, E. (2015). A new method of discriminating different types of post-Archean ophiolitic basalts and their tectonic significance using Th-Nb and Ce-Dy-Yb systematics. Geoscience Frontiers, 6, 481-501.

Shibata, T., & Yoshikawa M. (2004). Precise isotope determination of trace amounts of Nd in magnesium-rich samples. *Journal of the Mass Spectrometry Society of Japan*, 52, 317–324.

Schuster, R., & Stüwe, K. (2008). Permian metamorphic event in the Alps. *Geology*, 36, 603–606.

Sinigoi, S., Quick, J.E., Demarchi, G., & Klötzli, U.S. (2016). Production of hybrid granitic magma at the advancing front of basaltic underplating: Inferences from the Sesia Magmatic System (south-western Alps, Italy). *Lithos*, 252–253, 109–122.

Sloman, L.E. (1989). Triassic shoshonites from the Dolomites, Northern Italy: alkaline arc rocks in a strike-slip setting. *Journal of Geophysical Research*, 94, 4655-4666.

Spiess, R., Cesare, B., Mazzoli, C., Sassi, R., & Sassi, F.P. (2010). The crystalline basement of the Adria microplate in the eastern Alps: a review of the palaeostructural evolution from the Neoproterozoic to the Cenozoic. *Rendiconti Lincei*, 21, 31–50.

Stampfli, G.M. (2005). Plate tectonics of the Apulia-Adria microcontinents. Elsevier special volume "Crop Project – Deep Seismic exploration of the Central Mediterranean and Italy" (I. Finetti ed.), 747-766.

Sun, S.-s., & McDonough, W.F. (1989). Chemical and isotopic systematics of oceanic basalts: implications for mantle composition and processes. *Geological Society of London, Special Publication*, 42, 313-345.

Testa, B., Aldighieri, B., Bertini, A., Blendinger, W., Caielli, G., de Franco, R., … Kustatscher E. (2013). Geomorphodiversity of the San Lucano Valley (Belluno Dolomites, Italy): a Well-Preserved Heritage. *Geoheritage*, 5, 151–172.

Yoshikawa, M., & Nakamura, E. (1993). Precise isotope determination of trace amounts of Sr in Magnesium-rich samples. *Journal Of Mineralogy, Petrology and Economic Geology*, 88, 548–561.

Wilson, M., & Bianchini, G. (1999): Tertiary-Quaternary magmatism within the Mediterranean and surrounding regions. *Geological Society of London, Special Publication*, 156, 141-168.